Geant4/C++ Monte Carlo Studies of the BigBite Focal-Plane Detector System
DRAFT 0

J.R.M. Annand and D. Hamilton
Department of Physics and Astronomy
University of Glasgow
G12 8QQ Glasgow, SCOTLAND

22nd May 2001

Introduction

A model of the BigBite spectrometer [1, 2] has being designed within the framework of the C++ class library Geant-4 [3] for the purpose of calculating the necessary properties of the focal-plane detection system. At the present time the model is under development, but it is sufficiently advanced to give meaningful predictions of the necessary properties of the trigger-scintillator system. Normally this would provide only precise reference timing and particle identification information. However approved experiment E96-106 has proposed to use scintillators to provide a crude proton momentum reconstruction, in the expectation that the trigger detectors will be available before the final, high-rate MWPC tracking system is ready. Thus much of this preliminary draft deals with momentum reconstruction on the basis of scintillator position information only. Coding of a model of a possible MWPC tracker is in progress.

0.1 The BigBite Model

The model has been constructed with a view to study:

1. Particle identification in the trigger detectors by time of flight.
2. Particle identification in the trigger detectors by pulse height.
3. Emission-angle reconstruction using trigger-hit position information only.
4. Momentum reconstruction using trigger-hit position information only.
5. Momentum reconstruction by time of flight.
6. Emission-angle and momentum reconstruction with MWPC hit information. (Under construction).

0.1.1 Detector dimensions and the model geometry

Sectional views of the BigBite magnet are shown in Fig. 1 where the dimensions have been taken from the original NIKHEF/Budker engineering drawings. These dimensions have been coded into the Geant-4 model whose geometry is displayed in Fig. 2, along with the trajectories of 3 simulated proton events. A preliminary model of the dipole magnet assumes a constant field of 0.92 tesla within the volume outlined in magenta in Fig. 2. This volume is larger than the actual pole face, shown in dark blue in Fig. 1, to compensate for the fringing field beyond this region. The effective field boundaries (EFB), shown as dashed lines in Fig. 1, match the dimensions given in Ref. [1]. All calculations presented in this report assume that the magnet and detector system sit in partial vacuum. In reality the vacuum box will extend from the target to the auxiliary scintillator plane with the detectors probably sitting in a helium bag. This will be coded at a later stage.

The focal-plane trigger, as shown in Fig. 2, consists of 3 planes of plastic scintillator

1. The auxiliary plane in red, overall dimensions 1400×500×2 mm. As shown, it is segmented in the dispersive direction in 16 equal bars. Calculations have also been made for 32 or 64-way segmentation.
2. The main δE plane in green, overall dimensions 2000×500×3 mm. It is segmented in the dispersive direction into 15 equal + 1 half-width bars.
3. The main E plane in blue, overall dimensions 2000×500×30 mm. It is segmented in the dispersive direction into 15 equal + 1 half-width bars. The overlap of the δE and E planes gives 31 pixels in the dispersive direction. Calculations have also been made with 31 equal + 1 half-width segmentation in the δE and E planes, giving 63 pixels.

The scintillators are made of standard plastic scintillator, density 1.032 g.cm^{-3}, with an effective composition C_9H_{10}. The auxiliary plane sits just outside of the magnet coils (Fig.1) and the distance between the E and auxiliary planes, in the direction perpendicular to the exit EFB, is 900 mm.

All calculations have been made assuming isotropic particle emission within the limits $\theta \pm 80$ mr and $\phi \pm 300$ mr.

0.1.2 Software Technicalities.

The calculations have been performed on a variety of Intel-PIII platforms running RedHat 6.2 (Linux 2.2.14) and RedHat 7.1 (Linux 2.4.2). The Geant4 class library (version 4.3.1) and the BigBite model were compiled with the C++ compilers egcs 1.1.2 (RedHat 6.2) or gcc 2.96 (RedHat 7.1). For analysis purposes Geant4 has been linked with CERN Root version 3.00.06 [4]. Quantities calculated event by event have been saved in a root "tree", which is a generalisation of the "ntuple" concept employed in the HBOOK and PAW systems, and written to disk for subsequent Root analysis.

0.2 Preliminary Results

0.2.1 Particle identification by time of flight and pulse height

Each scintillator bar is assumed to be read by 2 photomultipliers (PM) so that the mean time of the PM signals is independent of position and the time difference gives the hit position along the scintillator bar (z-direction Fig.2). In the model individual PM timing is calculated for each hit as follows:

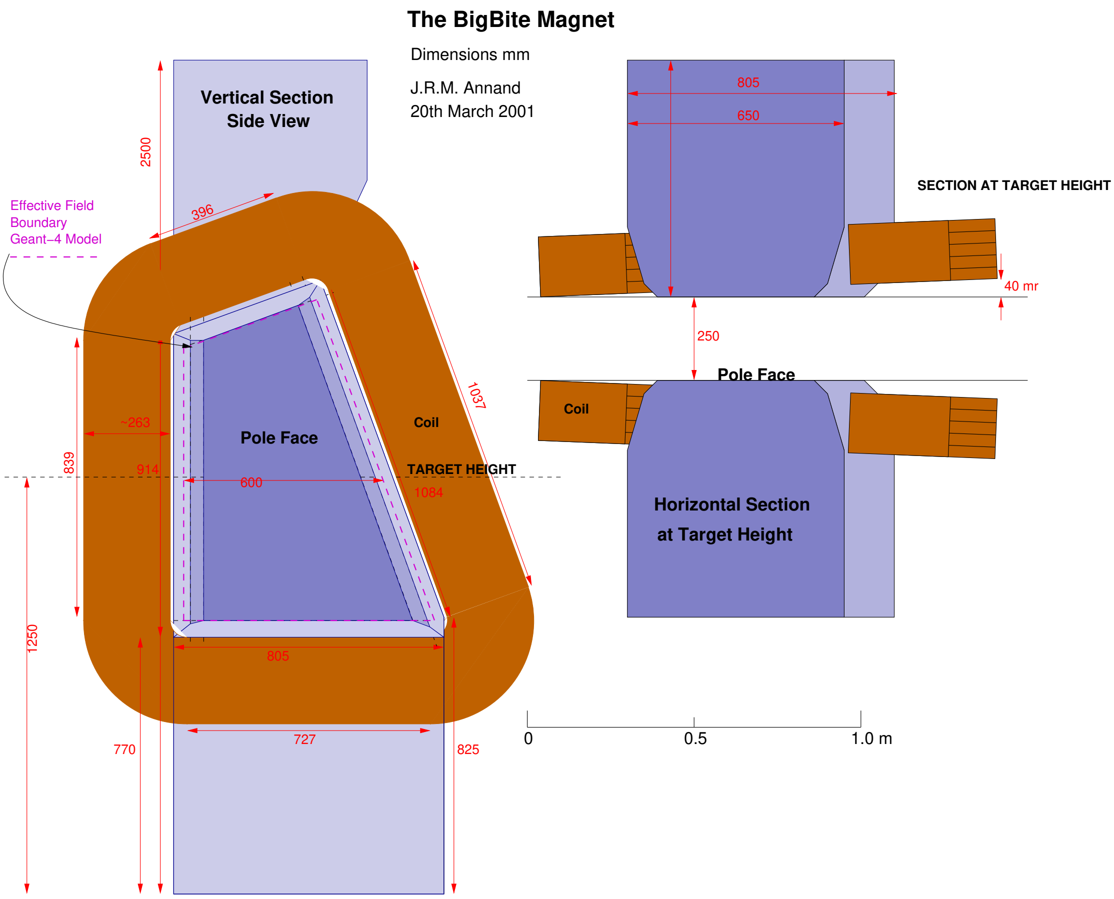

Figure 1: Views of the BigBite magnet

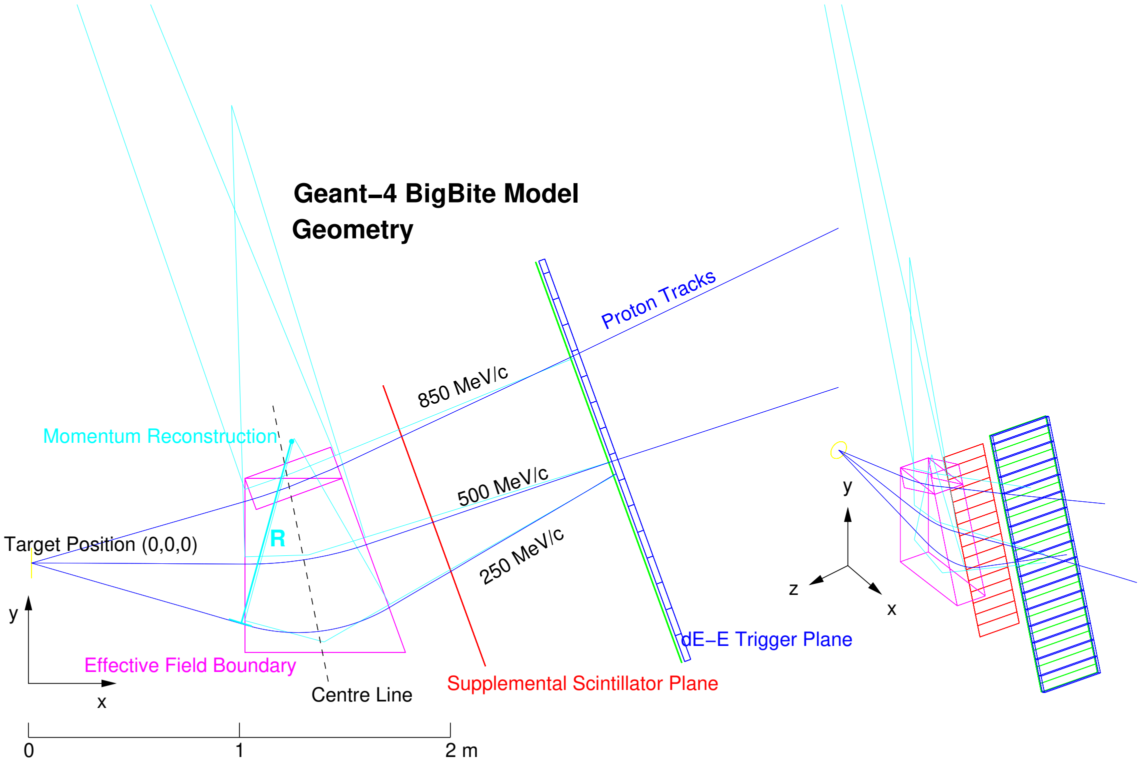

Figure 2: Graphical representation of the BigBite Geant4 model.

1. Determine the distances d_i from the hit position to the positions of the PM's at the ends of the scintillator bar.
2. The scintillation-light propagation time to each PM is $t_i = \frac{d_i}{v}$ where $v \approx \frac{2}{3}$c is the light velocity in the plastic.
3. Smear the propagation times t_i using a Gaussian pseudo-random number generator, assuming a resolution $\sigma = 150$ ps (350 ps FWHM).
4. The mean time $t_m = (t_1 + t_2)/2$ gives the "measured" hit time and the difference $t_1 - t_2$ gives the "measured" hit position.

Fig.3A shows the expected flight time between the auxiliary and E planes, as a function of momentum, for d, p, κ^+ and π^+. The projection of the flight times for momenta 800-900 MeV/c (Fig.3D) shows reasonable separation between d, p and unresolved κ^+ and π^+. The time difference shows the more-or-less linear relation between incident angle θ (to the spectrometer central line) and the "measured" hit position.

Energy loss in the rear $\delta E - E$ scintillators is displayed in Fig.3B. The distributions relating to κ^+ and π^+hits are contained within the dark region at the lower left of the plot. Average $\delta E/E$ energy loss for π^+ is $\sim 0.35/5.0$ MeV while the corresponding figures are $\sim 0.5/7.0$ MeV for κ^+. It can be seen that the E plane stops d of up to $\sim$80 MeV while the corresponding figure for p is $\sim$ 60 MeV. Work is in progress to account for finite resolution, non-linear scintillation response at high dE/dx and light attenuation in the scintillator bars. Optical photon transport within the plastic is being estimated in a separate Geant4 model, also under development..

0.2.2 Momentum resolution using scintillator-hit information only.

This issue has been investigated for varying degrees of segmentation of the trigger-scintillator planes:

1. 1400×350×**2** mm auxiliary plane in **16** elements, 2000×500×3, 30 mm δE-E planes each of **16** elements.
2. 1400×350×**2** mm auxiliary plane in **32** elements, 2000×500×3, 30 mm δE-E planes each of **16** elements.
3. 1400×350×**2** mm auxiliary plane in **64** elements, 2000×500×3, 30 mm δE-E planes each of **16** elements.
4. 1400×350×**2** mm auxiliary plane in **64** elements, 2000×500×3, 30 mm δE-E planes each of **32** elements.
5. 1400×350×**0.5** mm auxiliary plane in **64** elements, 2000×500×3, 30 mm δE-E planes each of **32** elements.

Cases 1-4 are intended for study of the dependence on trigger element width in the dispersive direction, while comparison of 4 and 5 shows the effects of multiple scattering in the auxiliary scintillator plane.

Proton momentum distributions are displayed for case 1 above in the "box" plots of Fig.4 as a function of the hit index (0-30) in the δE-E planes. The separate plots correspond to the hit index. labeled v1, in the forward auxiliary plane which is in the range 0-15. The vertical width of the pixels in each "line" denotes the number of counts in that pixel. It is immediately obvious that the widths of the momentum distributions corresponding to individual hit combinations are quite large.

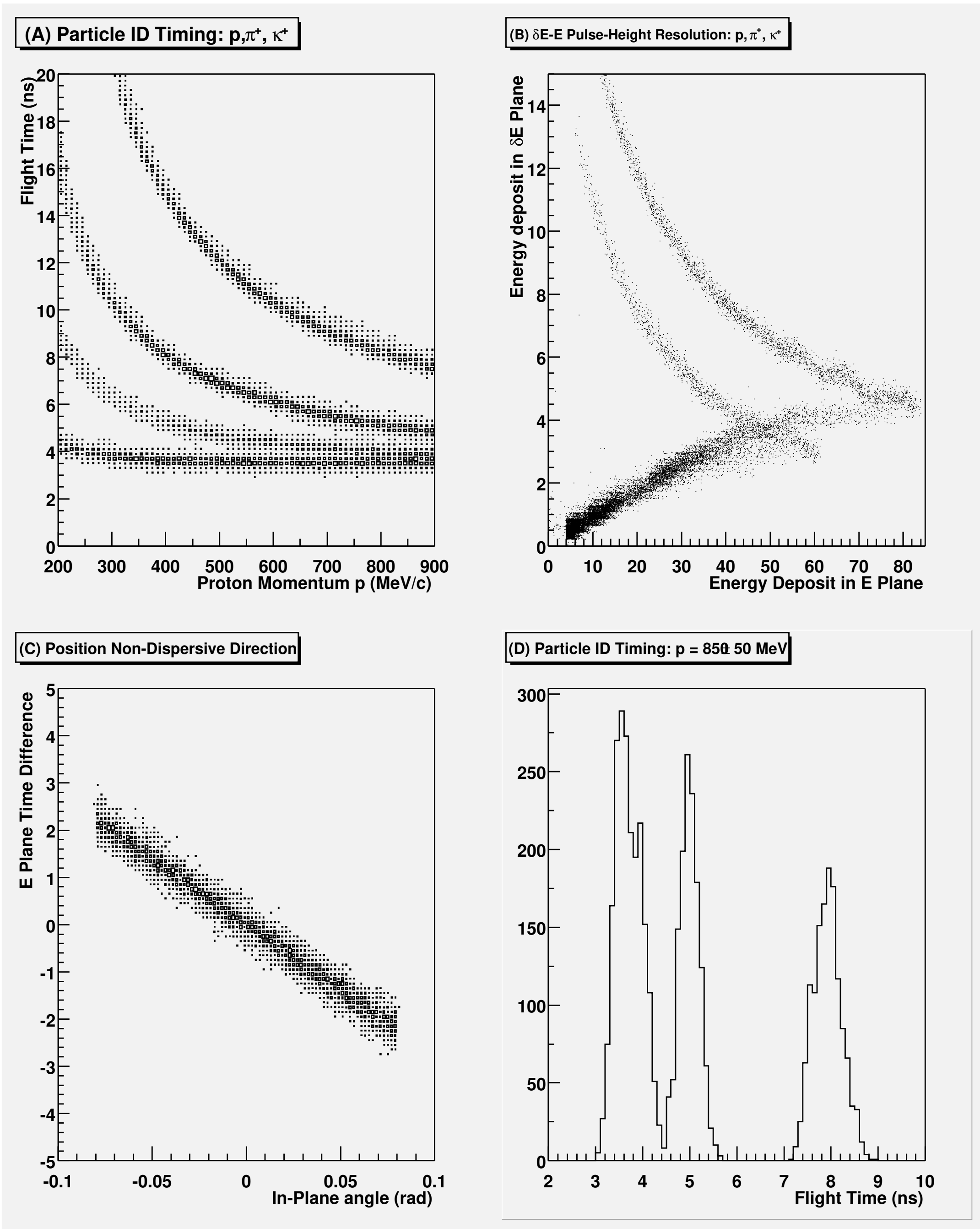

Figure 3: A) Flight time from auxiliary to δE-E scintillator planes for d(upper distribution), p and π^+(lower distribution); B) δE-E plots; C) Position info from E plane; D)Flight times for the momentum range 800-900 MeV/c. The right-hand distribution is due to protons while the left results from unresolved κ^+ and π^+.

To give a more quantitative idea of expected momentum resolution we have reconstructed the momentum on the basis of the exit track, according to the analytical method described in [1] and shown graphically in Fig.2. The line joining the hit positions in the scintillator planes is projected back to the exit effective field boundary (EFB) and the centre line of the magnet. The line joining the centre-line intersection and the target position defines the entrance track and its intersection at the entrance EFB is also recorded. The perpendicular projections at the entrance and exit EFB intersections join at a vertex (Fig.2) and the distance from the vertex to either of the EFB intersections gives the bend radius in the magnetic field. For the present calculations a thin target was assumed.

This procedure has been implemented event-by-event using:

- "exact" hit positions in the scintillator planes in order to gauge the accuracy of this 1st-order method and to estimate other contributions to resolution such as multiple scattering in the front auxiliary plane. The momentum reconstructed using this information is labeled p_0.
- the scintillator hit information which would be available in an experiment. In the dispersive direction this is taken as the centre of the pixel, while in the non-dispersive direction the time difference of the signals gives the position as outlined in subsections 0.2.1 and **??**. The momentum reconstructed using this information is labeled p_{sc}.

Fig.5 displays the intrinsic error of the reconstruction method, which will contain contributions due to the use of a first-order method as well as possible deficiencies of the MC model. The offsets of a few MeV/c from zero are under investigation. Comparison of the distribution widths for the cases of a 0.5 and 2 mm-thick auxiliary scintillator plane suggest that a substantial contribution arises in the latter from multiple scattering in that plane.

Fig.6 displays the error in momentum reconstructed from scintillator position information, as a function of momentum, while Fig.7 and 8 show vertical sections of these 2D distributions taken at $p = 300$ MeV/c and $p = 600$ MeV/c respectively. These plots have been made for the full out-of-plane angle range of ± 300 mr. The dependence of the relative error in reconstructed momentum $(p - p_{sc})/p$ on this angle is shown in Fig.9 for a momentum $p = 600$ MeV/c.

0.2.3 Angular Reconstruction and Acceptance

This work is proceeding in parallel with the construction of a model of the MWPC tracking systems. An idea of θ resolution using scintillators only may be gauged from Fig.10 where the resolved peaks correspond to incident-particle angles of -70, 0, +70 mr with respect to the central line through the spectrometer. The dependence of time difference on incident angle is displayed in Fig.3. Both calculations assume a time resolution $\sigma = 150$ ps (subsection 0.2.1). A full reconstruction of the incident track will be made when the MWPC model is in place.

The reconstruction of the out-of-plane angle ϕ, also displayed in Fig.10, is an additional product of the analytical procedure described in subsection 0.2.2. The reconstructed angle ϕ_0 is the result of using exact hit coordinates in the focal-plane detectors while ϕ_{sc} is produced by the simulated experimental position produced by a scintillator bar.

Out-of-plane acceptance for the actual, as opposed to reconstructed, angle is displayed in Fig.11 for the focal plane geometry given in subsection 0.2.2 (case 2) and displayed in Fig.2. A and B show the hit distributions in the auxiliary and δE-E scintillator planes respectively. C shows the hit distribution as a function of ϕ and p for coincident hits in the auxiliary and δE-E planes while D is a similar display for hits in the auxiliary plane, irrespective of whether the δE-E plane is hit or not. It is evident that the δE-E plane does not quite match the coverage of the auxiliary plane at low p, large positive ϕ and high p, large negative ϕ. Full coverage over the full momentum range would require enlargement of the δE-E layer or reduction of the flight path between the layers.

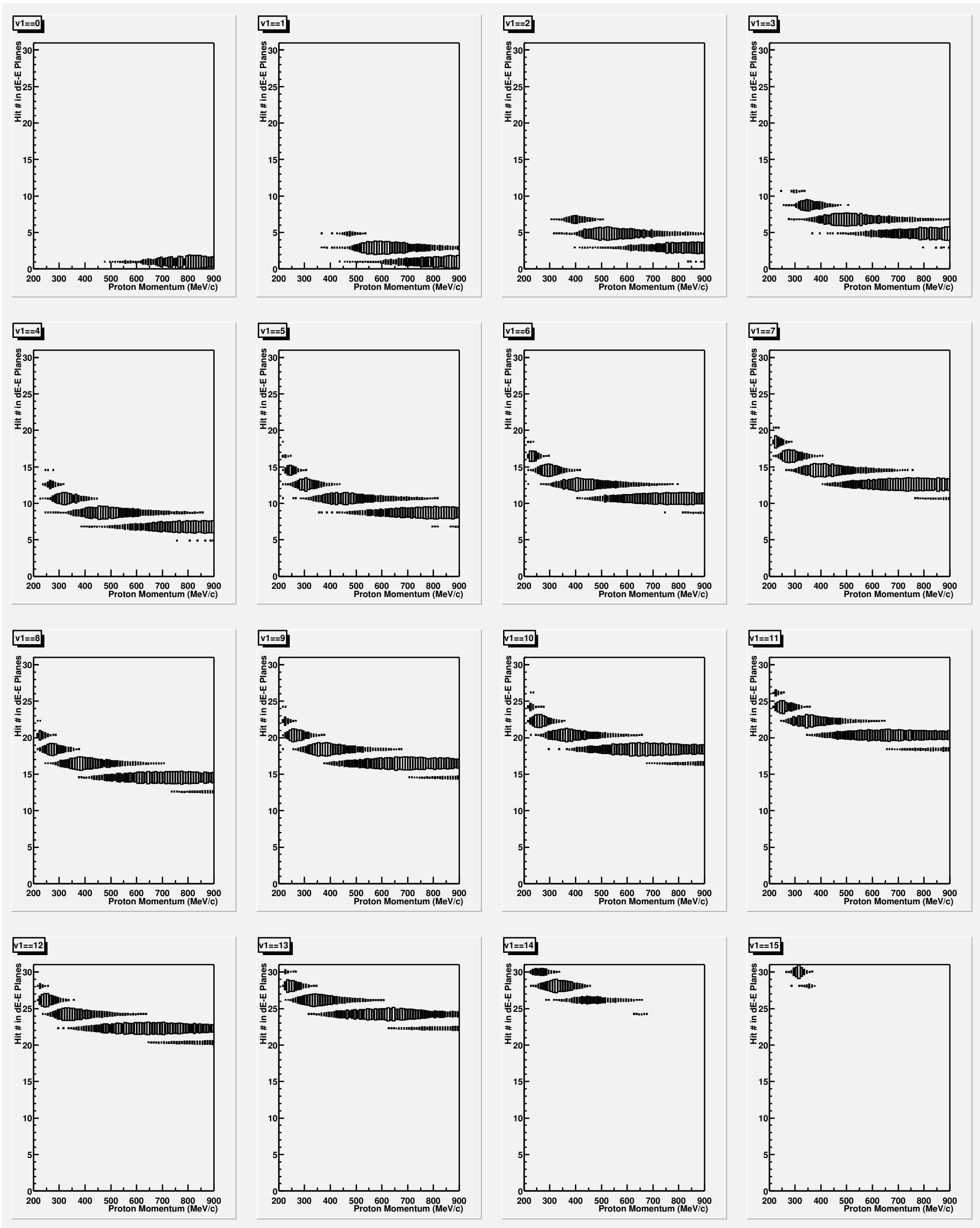

Figure 4: Proton momentum distributions for hits in each of the 16 elements of the auxiliary scintillator plane. Each plot shows the proton momentum distribution for corresponding hits in the 31 pixels of the main δE-E trigger plane. The out-of-plane angle range is ±300 mr.

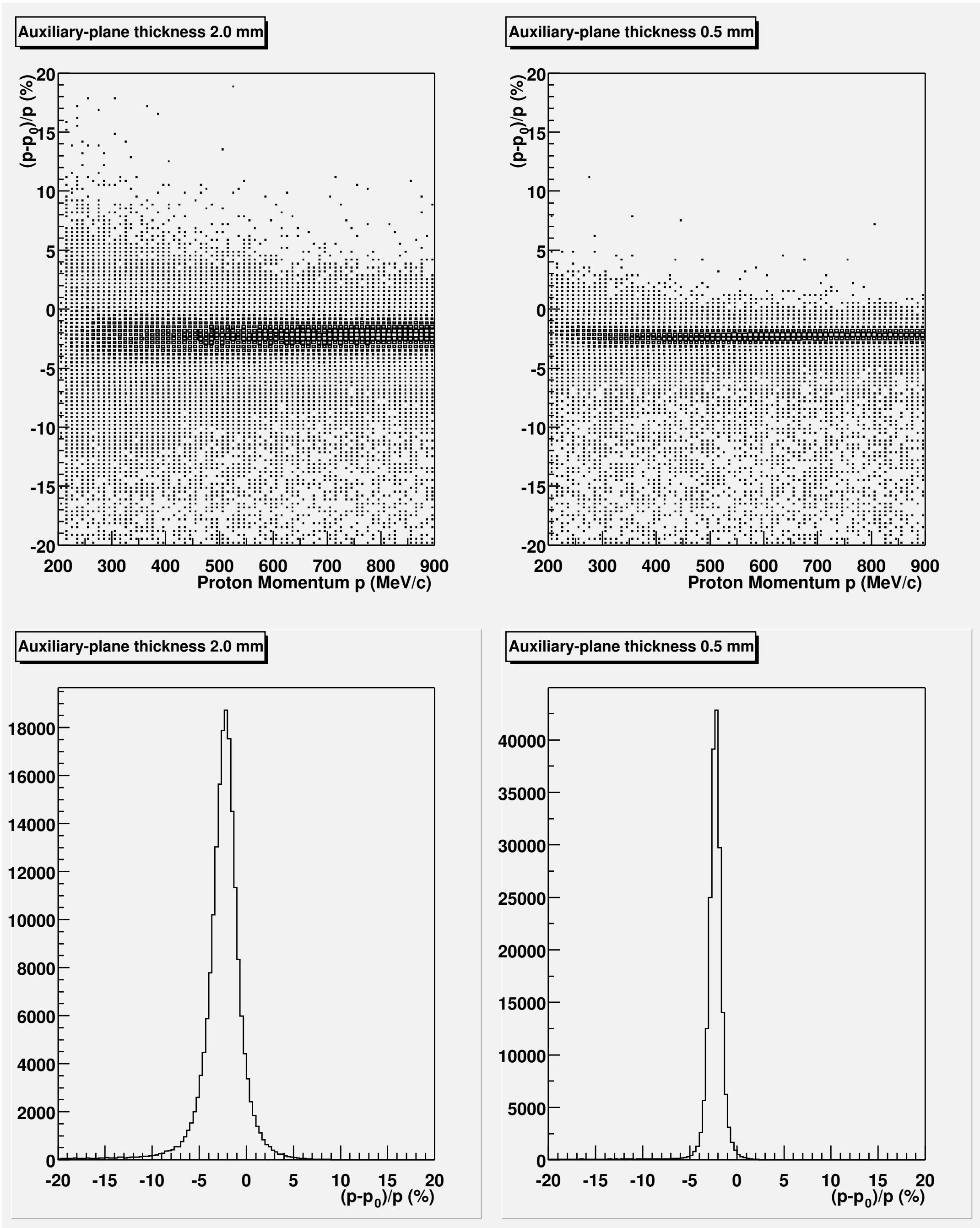

Figure 5: Momentum reconstructed on the basis of exact hit position in focal-plane detector.

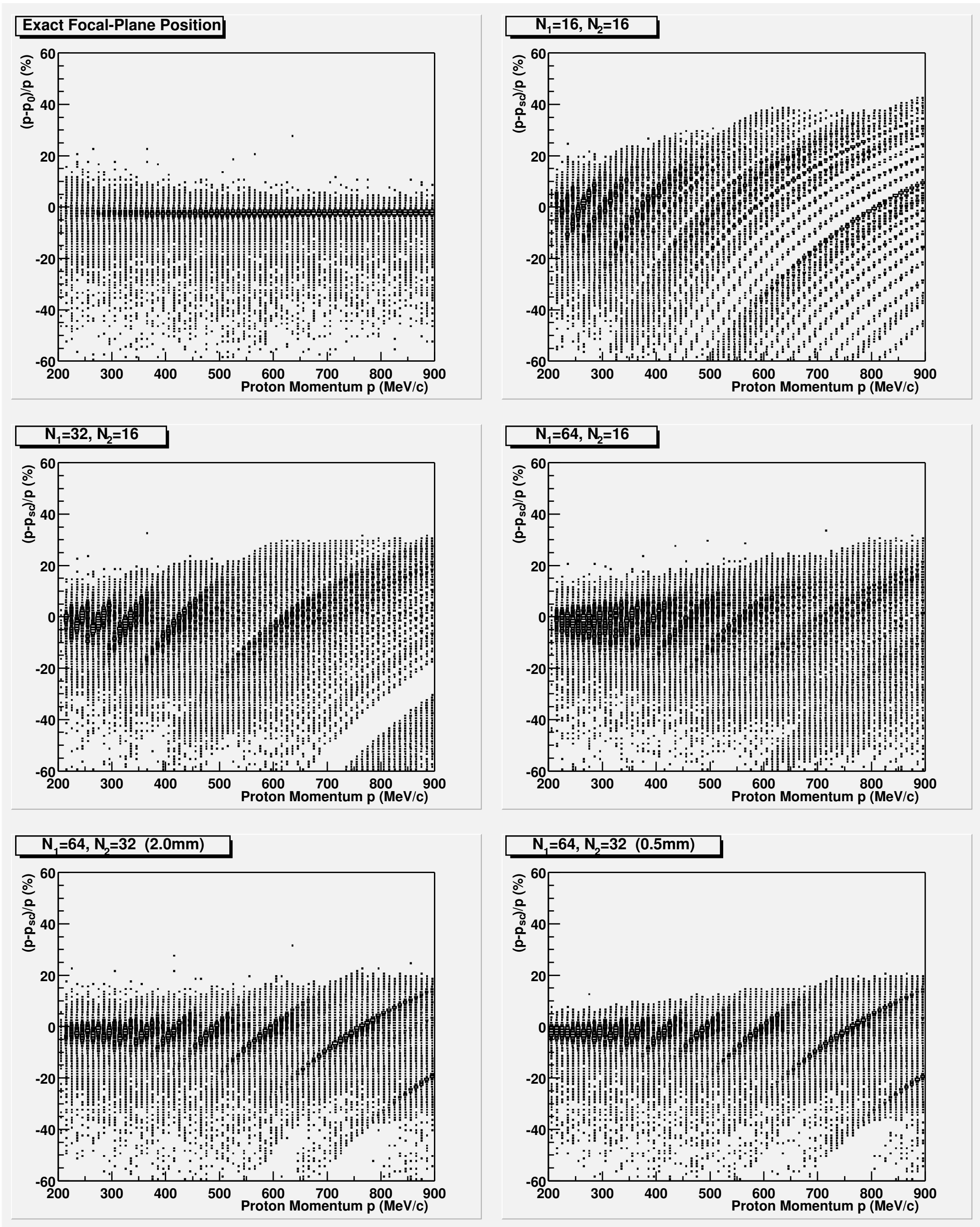

Figure 6: Error in reconstructed momentum for various scintillator configurations. Out-of-plane angle range ±300 mr.

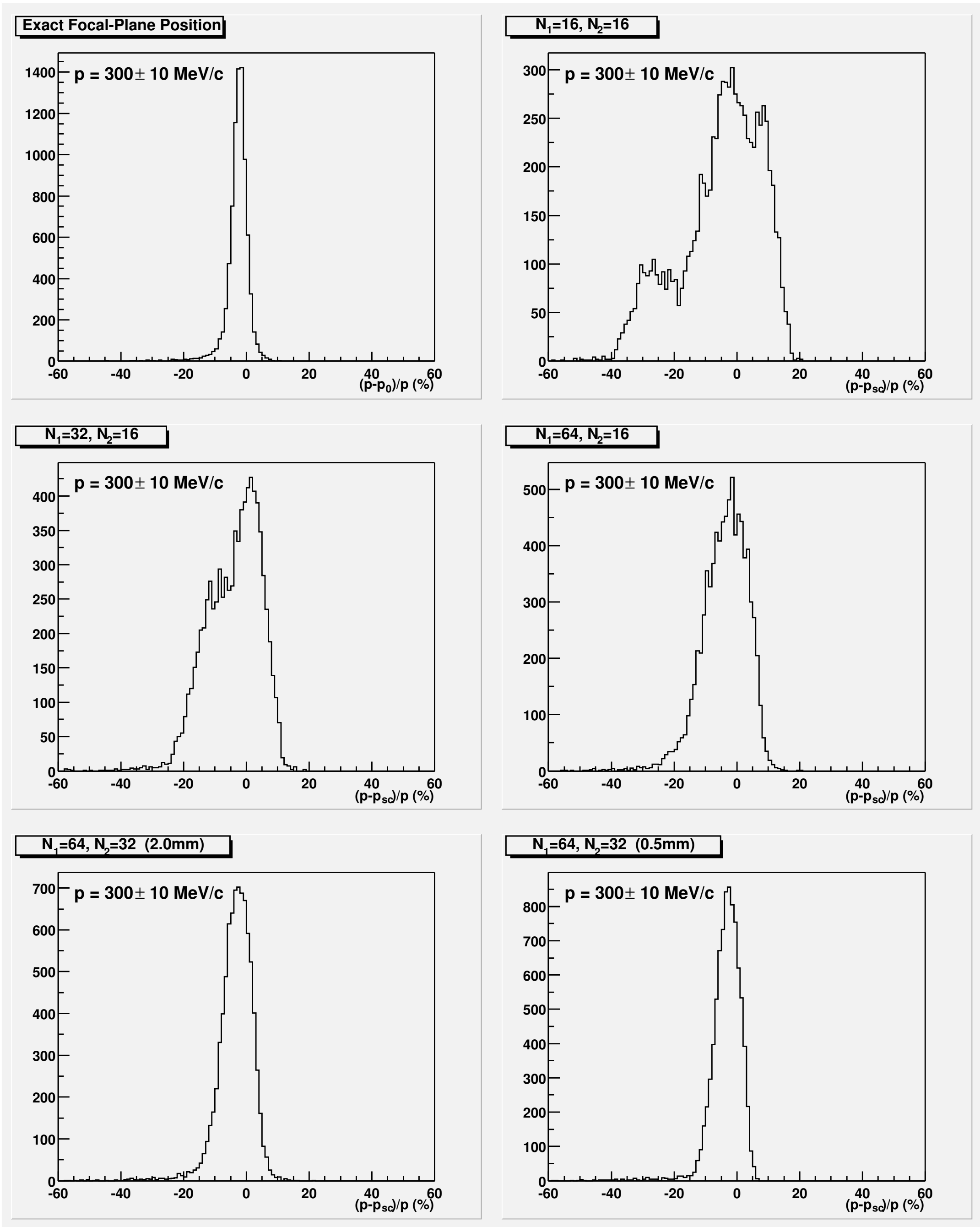

Figure 7: Error in reconstructed momentum for various scintillator configurations. Out-of-plane angle range ±300 mr.

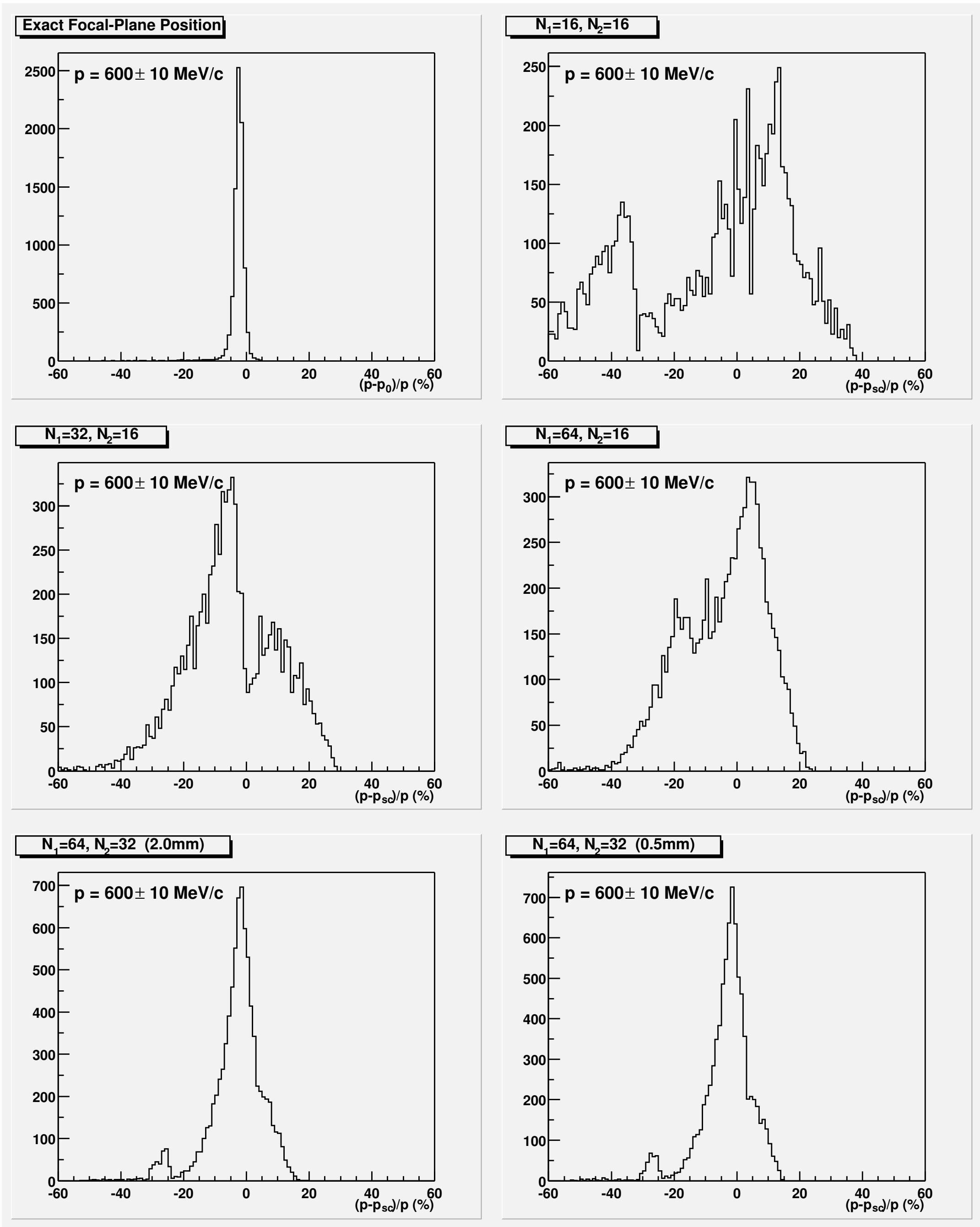

Figure 8: Error in reconstructed momentum for various scintillator configurations. Out-of-plane angle range ±300 mr.

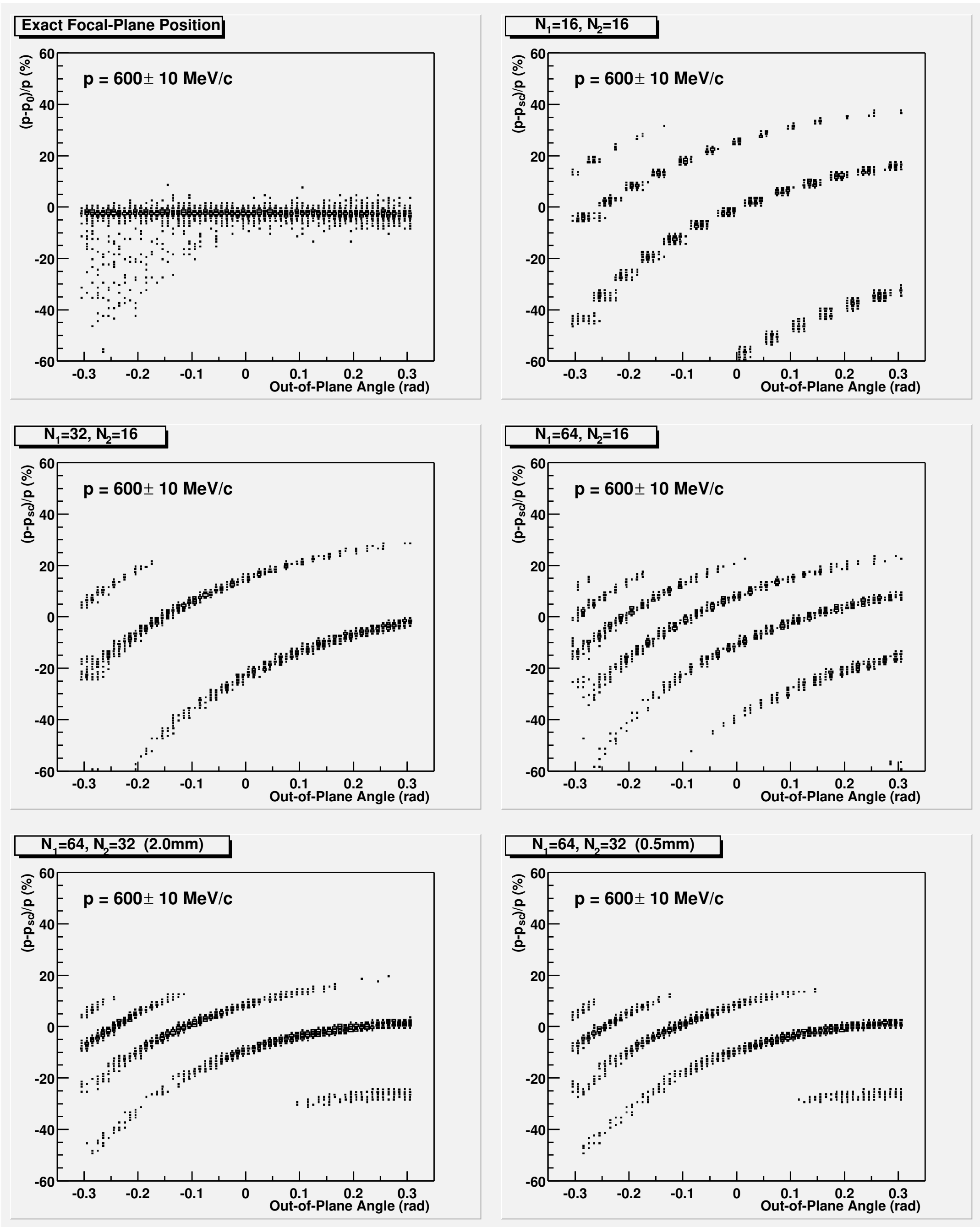

Figure 9: Error in reconstructed momentum at p = 600 MeV/c for various scintillator configurations as a function of out-of-plane angle.

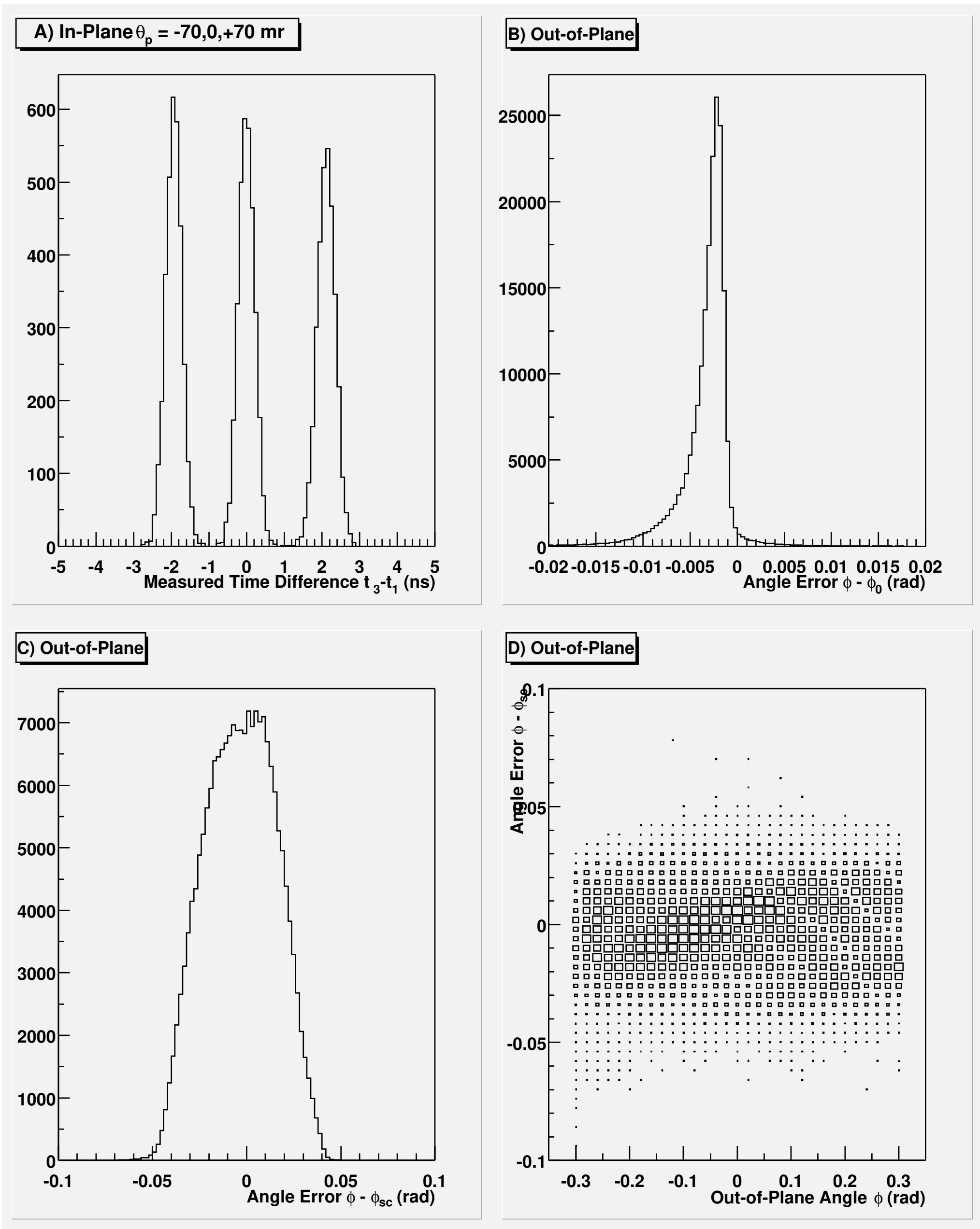

Figure 10: Reconstruction of θ and ϕ.

Alternatively if experiments do not require 200-900 MeV/c coverage then a little flexibility in the mounting position of the focal-plane system would suffice. Note that with a 2 mm-thick auxiliary layer 200 MeV/c protons do not penetrate to the E-layer causing the horizontal cut off at $\sim$ 210 MeV/c in C. 200 MeV/c is obtainable with a 0.5 mm thick auxiliary layer.

The present focal-plane geometry gives full $\pm$ 80 mr coverage in θ.

0.2.4 Momentum Reconstruction using Time of Flight.

With a PM timing resolution of $\sigma \sim$ 150 ps and a flight path of 900 mm Time of Flight (TOF) gives some supplemental momentum resolution as well as very useful particle identification. The particle velocity has been obtained from the difference of the mean times (subsection 0.2.1) for hits on the auxiliary and E scintillator planes and the flight path between the hits. For the flight path determination the non-dispersive hit coordinate is obtained from the PM time difference while the dispersive corrdinate is just the mid-point of the scintillator bar. Fig.12A displays the difference between the actual momentum p and the TOF reconstructed momentum p_{tof} as a function of p, while B,C and D show vertical sections of this plot at selected momenta.

0.3 Conclusion

16-way segmentation of the auxiliary scintillator plane seems a bit too crude. Increasing this to 32-way will increase the cost by almost a factor 2.

More results still to come!!

References

[1] *The optical properties of the BigBite spectrometer at NIKHEF*, D.J.J. de Lange et al., Nucl. Instr. and Meth. **A412**(1998),254.

[2] *A large acceptance spectrometer for the internal target facility at NIKHEF*, D.J.J. de Lange et al., Nucl. Instr. and Meth. **A**406(1998),182.

[3] *Geant4 user's guide for application developers*, Version 4.3.0 December 2000, see CERN software repository `http://wwwinfo.cern.ch`

[4] *Root users guide v0.7*, January 2001, see `http://root.cern.ch`

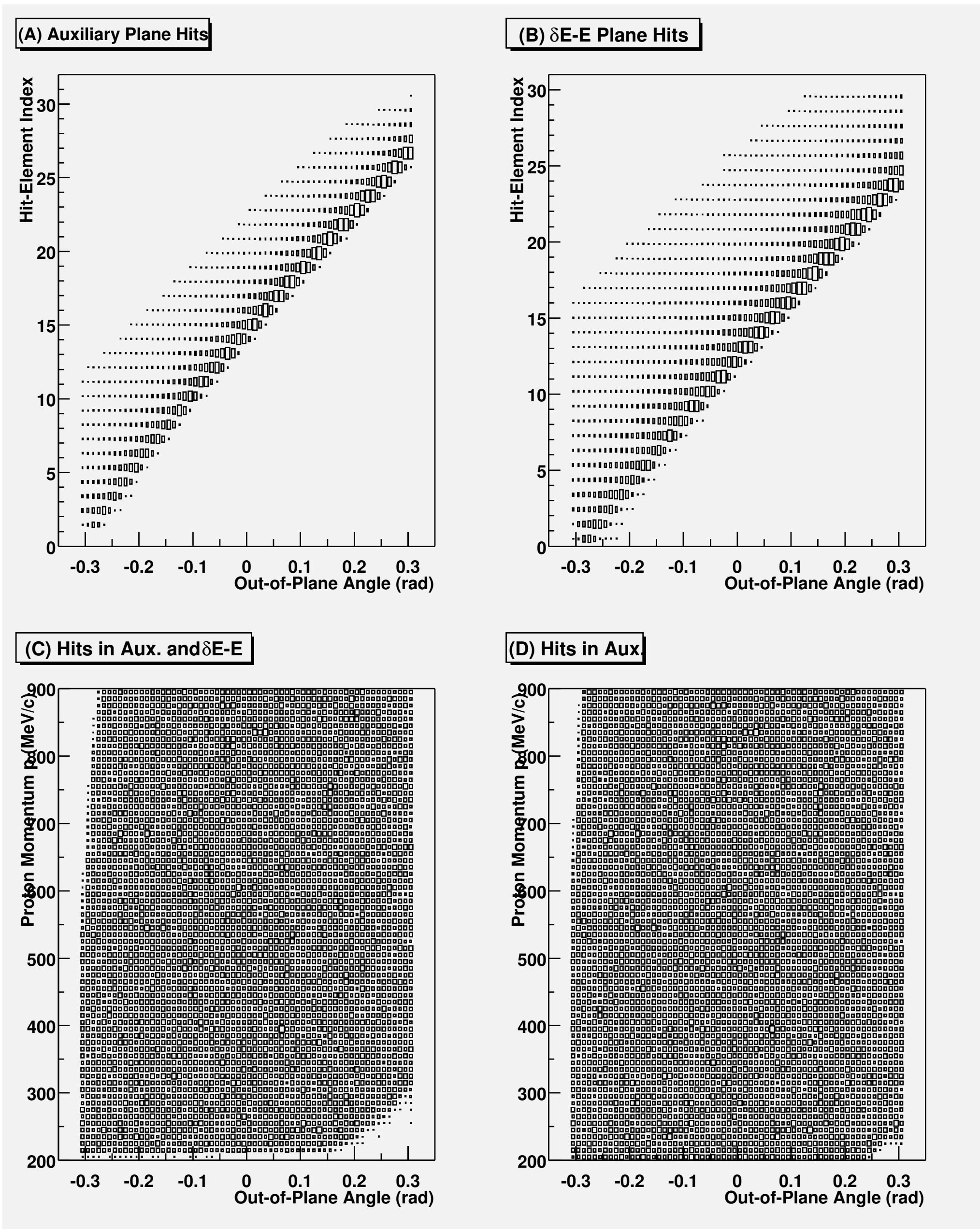

Figure 11: Angular acceptance using the present focal-plane geometry.

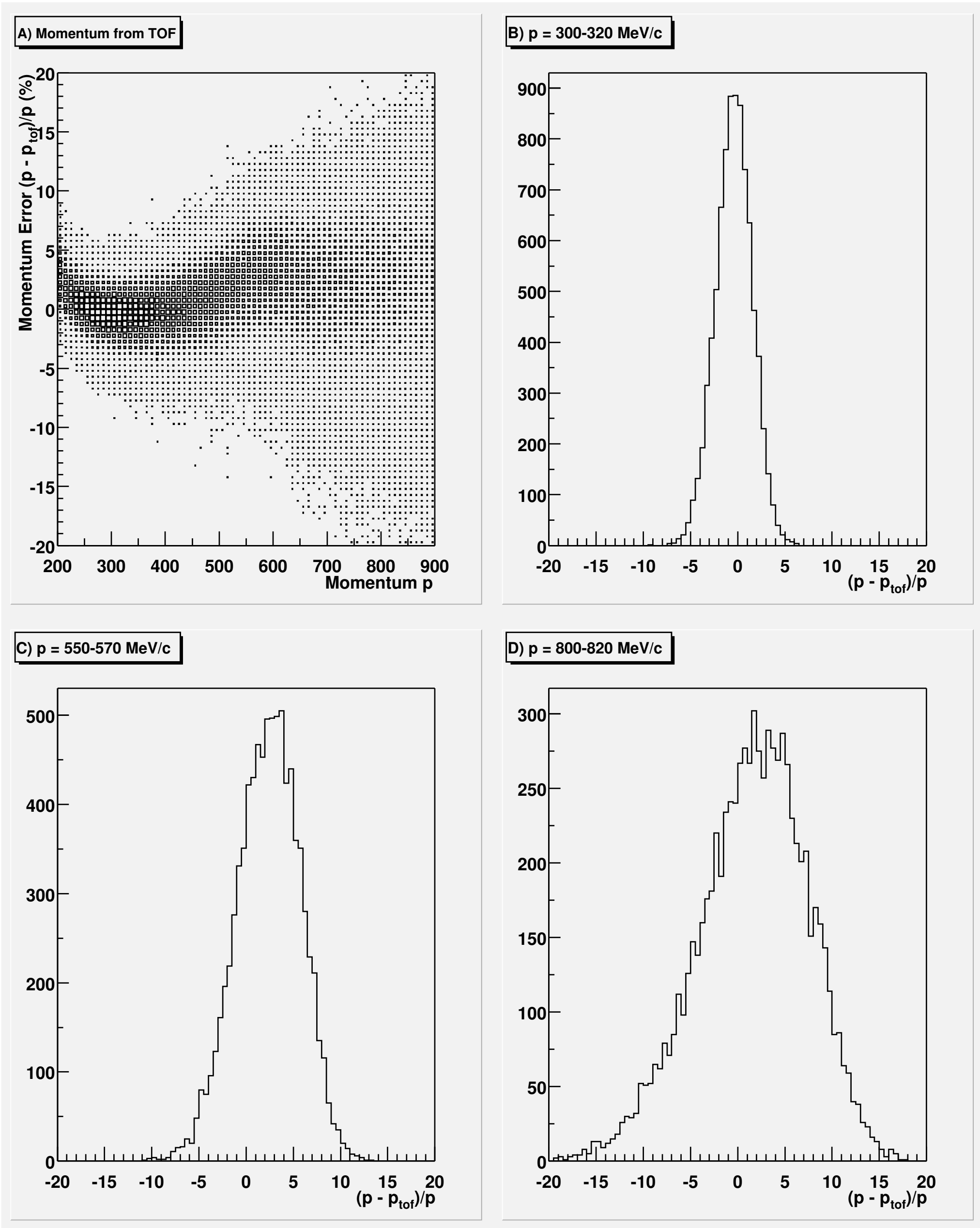

Figure 12: Momeuntum reconstruction from time of flight